The photoreactions of the carboxylate complexes of 5,10,15,20-tetra(2-N-methylpyridyl)porphyrin

Bruce C. Gilbert [a], George R. Hodges [a], John R. Lindsay Smith [a,*], Philip MacFaul [a], Philip Taylor [b]

[a] *Department of Chemistry, University of York, York YO1 5DD, UK*
[b] *Decorative Research and Development, ICI Paints plc, Wexham Road, Slough, Berkshire SL2 5DS, UK*

Abstract

Anaerobic aqueous solutions of a selection of alkyl and substituted alkylcarboxylic acids, in the presence of iron(III) 5,10,15,20-tetra(2-N-methylpyridyl)porphyrin, have been irradiated with light ($\lambda > 390$ nm). In all the reactions this brought about the photolysis of an iron(III) porphyrin–carboxylate complex (monitored by UV–vis spectroscopy) to give the iron(II) porphyrin and carboxyl radical. The fate of the carboxyl radical, following decarboxylation, has been investigated by EPR spectroscopy using spin-traps. These studies show that substituents have a marked influence on the rate and course of the reactions. In the presence of dioxygen the system is catalytic since the iron(II) porphyrin is rapidly oxidised to the iron(III) species. Supporting the catalyst on silica gel greatly improves the stability of the catalyst to self oxidation (bleaching).

Keywords: Carboxylic acid; Catalysis; Decarboxylation; EPR spectroscopy; Iron(III) porphyrin; Photoreduction; Spin trapping

1. Introduction

The widely studied redox cleavage of the axial ligand–iron bond of iron(III) porphyrins can be brought about either thermally [1] or under the influence of light [2–7] (Scheme 1). The former reaction is thought to be important in the iron(III) porphyrin catalyzed oxidation of hydrocarbons by dioxygen developed by Ellis and Lyons [8]. The latter has been used to bring

about reactions with a range of carbon, nitrogen, oxygen and halogen centred radicals [3–7,9].

In this paper we describe some of our studies on the photoreduction of iron(III)tetra(2-N-methylpyridyl)porphyrin (Fe^{III}T2MPyP) (Fig. 1) by alkyl and substituted alkylcarboxylic acids in aqueous and acetonitrile solution.
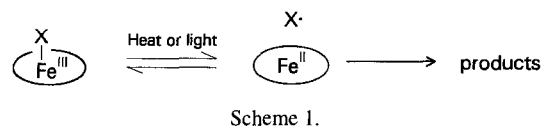
2. Results and discussion

2.1. The photosystem

The photoreactions were carried out with anaerobic solutions of the carboxylic acid (0.1 M) and Fe^{III}T2MPyP (10^{-4} for EPR studies

Scheme 1.

Fig. 1. Iron(III) 5,10,15,20-tetra(2-N-methylpyridyl)porphyrin.

and 10^{-5} M for UV–vis and product studies) using light of wavelength > 390 nm. The extent and rate of photoreduction of the iron(III) porphyrin was readily monitored by UV–vis spectroscopy. This showed the clean conversion of the iron(III) to iron(II) porphyrin with sharp isosbestic points (for example, Fig. 2). Introducing air into the solutions at the end of the photoreduction led to the complete regeneration of the Fe^{III}T2MPyP.

The photoactive region of the spectrum of the Fe^{III}T2MPyP–carboxylate complexes was examined using the photoreaction of pivalic acid and a selection of light filters (> 390 nm, 420–460 nm, 460–530 nm and > 580 nm). This showed that the iron(II) porphyrin was formed in all the reactions, except that in which light with wavelength shorter than 580 nm was absent. The initial rates of reaction were 25×10^{-8}, 1.8×10^{-8} and 0.5×10^{-8} mol s^{-1} for
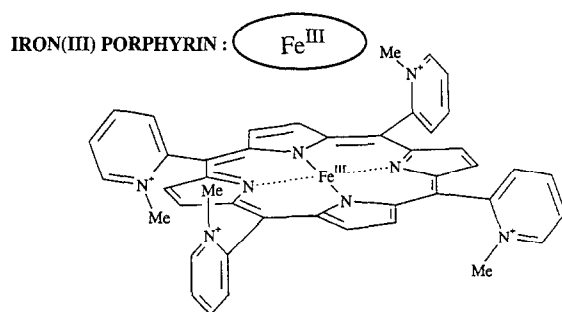
the filters > 390 nm, 420–460 nm and 460–530 nm, respectively. The photoreduction occurs when the irradiation is in the region of the ligand to metal charge transfer band [3], suggesting that for the carboxylate complexes of Fe^{III}T2MPyP this lies within the Soret peak of the UV–vis spectrum.

Photoreactions in the presence of air did not lead to the build-up of Fe^{II}T2MPyP; instead the iron(III) porphyrin was slowly bleached (Fig. 3). In these reactions dioxygen rapidly regenerates Fe^{III}T2MPyP from the iron(II) porphyrin, however, a minor oxidative side reaction that
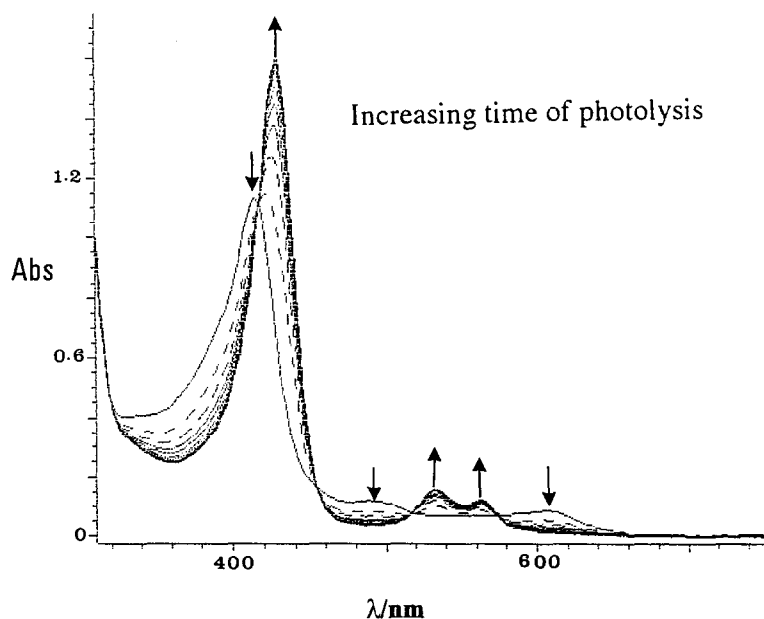

Increasing time of photolysis

Fig. 2. UV–vis spectrum of the anaerobic photoreaction of Fe^{III}T2MPyP and phenylacetic acid in acetonitrile solution showing the build-up of Fe^{II}T2MPyP with increasing time (0–300 s).
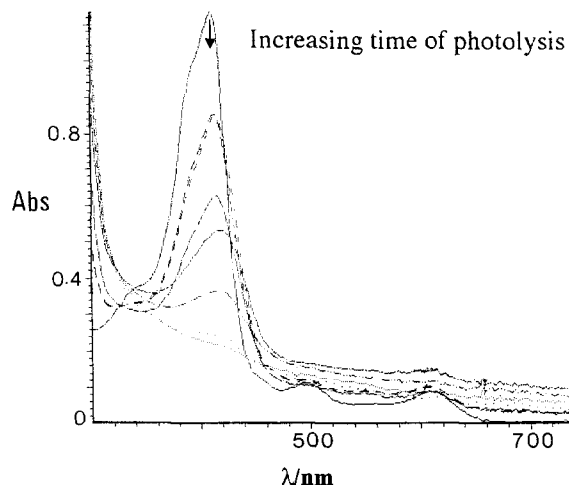
Fig. 3. UV–vis spectrum of the aerobic photoreaction of $Fe^{III}T2MPyP$ and phenylacetic acid in aqueous solution showing the slow bleaching of the iron(III) porphyrin with increasing time.

Fig. 5. The time dependent build-up of $Fe^{II}T2MPyP$ in the anaerobic photoreactions of $Fe^{III}T2MPyP$ in aqueous solution. (●) Pivalic acid, (♦) 2-methylpropanoic and phenylacetic acids, (▲) propanoic acid, (■) acetic acid.

accompanies the reoxidation leads to the slow loss of the iron(III) porphyrin catalyst.

The fate of the carboxyl radicals formed in the photoreactions was determined by EPR spectroscopy using the spin traps DMPO and DBNBS (Fig. 4). Also, in selected photocatalyzed oxidations in the presence of air, the products were analyzed and quantified by gas chromatography.

2.2. Alkyl- and aralkyl-carboxylate complexes

The rates of the photoreduction of $Fe^{III}T2MPyP$ by phenylacetic and a selection of

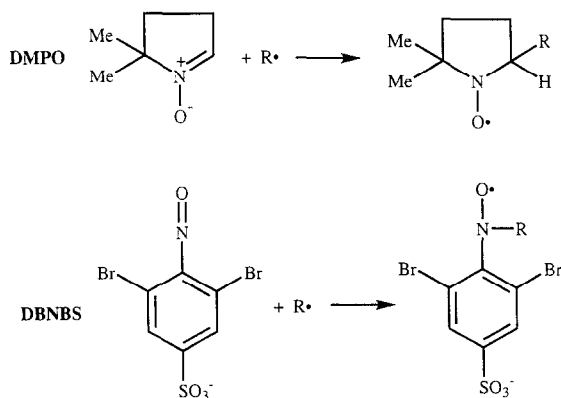alkylcarboxylic acids showed a strong dependence on the structure of the acids (Fig. 5). These correlate well with the known rates of decarboxylation of the carboxyl radicals (Table 1). We suggest that this arises from the recombination of the $Fe^{II}T2MPyP$ and carboxyl radical, formed within a solvent cage, competing with the decarboxylation (Scheme 2). Consequently, assuming the rate of the back reaction is approximately the same for all the carboxyl radicals, the faster the decarboxylation, the faster the rate of formation of $Fe^{II}T2MPyP$.

The carbon radicals formed by the decarboxylation were trapped with DMPO and

Fig. 4. Spin traps used in the EPR identification of radicals in the photoreactions of $Fe^{III}T2MPyP$-carboxylate complexes.
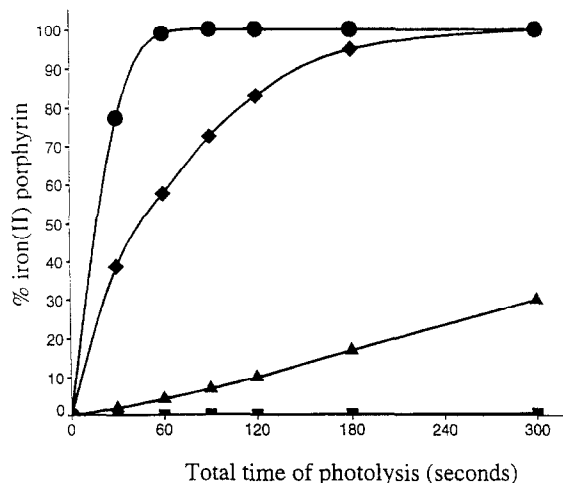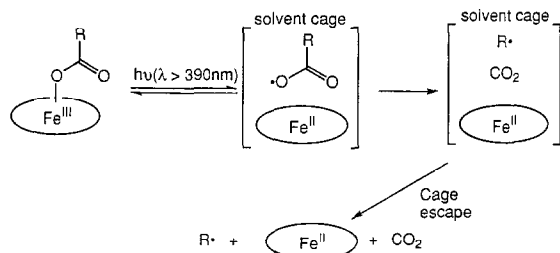
Table 1

Initial rates of photoreduction of $Fe^{III}T2MPyP$ by alkylcarboxylic acids and by phenylacetic acid, in anaerobic aqueous solution [a], and rates of decarboxylation of carboxyl radicals

Carboxylic acid	Initial rate of $Fe^{II}T2MPyP$ formation $(10^{-8}$ mol $s^{-1})$	Rate of decarboxylation of carboxyl radical [10] $(10^9$ $s^{-1})$
Me_3CCO_2H	25	11
Me_2CHCO_2H	13	6.5
$PhCH_2CO_2H$	13	5
$MeCH_2CO_2H$	0.9	2
$MeCO_2H$	0.3	< 1.3

[a] $[Fe^{III}T2MPyP] = 1 \times 10^{-5}$ M; [carboxylic acid] = 0.1 M; pH = 2.9.

Scheme 2.

$R^1 = Me$
$R^2 = H$ } $X = Br$ or Cl

$R^1 = R^2 = Me$, $X = Br$ or OH
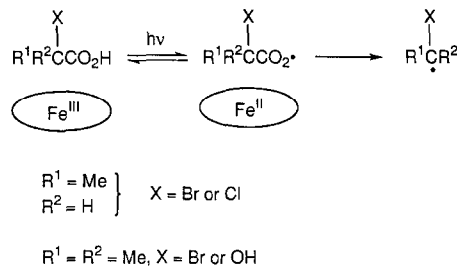
Scheme 3.

DBNBS and the adducts were identified by EPR spectroscopy (Table 2).

The scope of the photodecarboxylation with $Fe^{III}T2MPyP$ was investigated further with a selection of α-, β-, and γ-substituted carboxylic acids. This revealed that photocleavage with light (> 390 nm) is a general phenomenon for the $Fe^{III}T2MPyP$–carboxylate complexes. However, the subsequent reactions following decarboxylation are sensitive to the substituent, in particular when the resulting radicals are susceptible to redox reactions (vide infra).

2.3. α-hydroxy- and α-halo-alkylcarboxylate complexes

The photoreactions of two hydroxyacids, glycolic and 2-hydroxy-2-methylpropanoic acid,

and three haloacids, 2-chloropropanoic, 2-bromopropanoic and 2-bromo-2-methylpropanoic acid, were investigated (Scheme 3). The fastest reactions occurred with the α-hydroxyacids (initial rates: $HOCH_2CO_2H$, 8×10^{-8} mol s^{-1} and $HOCMe_2CO_2H$, 11×10^{-8} mol s^{-1}). This is to be expected since not only will the hydroxyl group stabilise the carbon radical formed by decarboxylation but also the radical will rapidly reduce a further molecule of $Fe^{III}T2MPyP$ [11].

The build-up of iron(II) in the reactions of the haloacids is slower for two reasons. First, the halo-groups do not stabilise the radicals following decarboxylation (cf. bond dissociation energies of the C–H bond in methanol

Table 2
Hyperfine splittings and assignments of radical adducts of DMPO and DBNBS from photoreactions of $Fe^{III}T2MPyP$ with alkylcarboxylic acids and phenylacetic acid in anaerobic aqueous solution [a]

Carboxylic acid	Spin trap	Hyperfine splittings (mT)		Assignment of trapped radical
		a_N	a_H	
Me_3CCO_2H	DMPO	1.625	2.320	$Me_3C^{\cdot}$
	DBNBS	1.425	0.066	$Me_3C^{\cdot}$
			0.038	
Me_2CHCO_2H	DMPO	1.625	2.425	$Me_2CH^{\cdot}$
	DBNBS	1.424	0.959	$Me_2CH^{\cdot}$
$MeCH_2CO_2H$	DMPO	1.615	2.310	$MeCH_2^{\cdot}$
	DBNBS	1.424	1.260	$MeCH_2^{\cdot}$
			0.068	
			0.033	
$MeCO_2H$	DMPO	1.615	2.295	$Me^{\cdot}$
		1.438	1.340	$Me^{\cdot}$
$PhCH_2CO_2H$	DMPO	1.600	2.240	$PhCH_2^{\cdot}$
	DBNBS	1.438	1.178	$PhCH_2^{\cdot}$
			0.068	

[a] g-value 2.0060 ± 0.0001. $[Fe^{III}T2MPyP] = 1 \times 10^{-4}$ M; $[RCO_2H] = 0.1$ M; [spin trap] $= 5 \times 10^{-2}$ M; pH $= 2.9$.

Scheme 4.

Scheme 5.
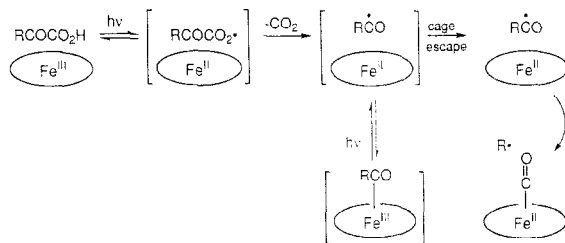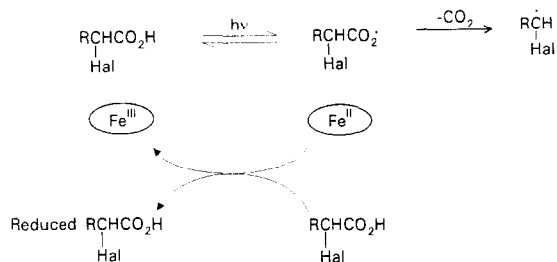
chloromethane and bromomethane, 393, 431 and 431 kJ mol^{-1}, respectively [12]) but, more importantly, the Fe^{II}T2MPyP reacts with the haloacid substrate regenerating the iron(III) porphyrin. Indeed the reactions go to an equilibrium, rather than to completion, where the photochemical generation of iron(II) equals its rate of oxidation by the substrate (Scheme 4).

2.4. Ketoacid complexes

The photoreaction of the α-ketoacid, 3-methyl-2-oxobutanoic acid, with Fe^{III}T2MPyP rapidly gave the expected shift in the Soret peak from 412 to 426 nm. However, unlike the alkyl carboxylic acids, the UV–vis spectrum showed that with further illumination a new species (Soret peak 418 nm) was formed. Introduction of air into the reactions before or after the formation of the 418 nm species regenerated the spectrum of Fe^{III}T2MPyP. The reaction carried out in the presence of DMPO showed the presence of two adducts from carbon-centred radicals which we attribute to an acyl (Me_2CHĊO)

and an alkyl (Me_2ĊH) radical formed by sequential decarboxylation and decarbonylation (Fig. 6, Scheme 5). We suggest the initial photodecarboxylation generates an acyl–iron porphyrin complex which on further illumination gives the alkyl radical and the Fe^{II}T2MPyP–CO complex. The identity of the latter species, with Soret peak at 418 nm, was confirmed by comparison with the UV–vis spectrum of an authentic solution of the CO complex prepared by passing CO into an anaerobic aqueous solution of Fe^{II}T2MPyP obtained by photoreduction of Fe^{III}T2MPyP by pivalic acid.

The rate of the photoreaction of the β-ketoacid, acetone dicarboxylic acid (monitored by UV–vis spectroscopy), appeared to be very slow since negligible Fe^{II}T2MPyP was formed even after 25 min illumination. However, the reaction generated substantial CO_2 and when carried out in the presence of DMPO gave an EPR signal which we attribute to the DMPO–ĊH$_2$COCH$_2$CO$_2$H adduct. We account for these observations by assuming that decarboxylation
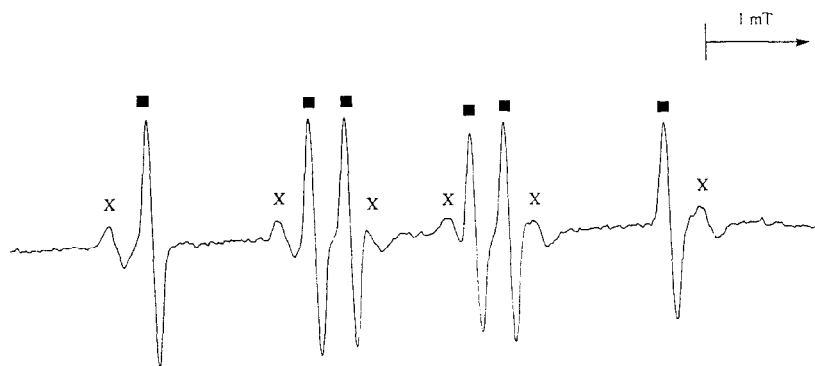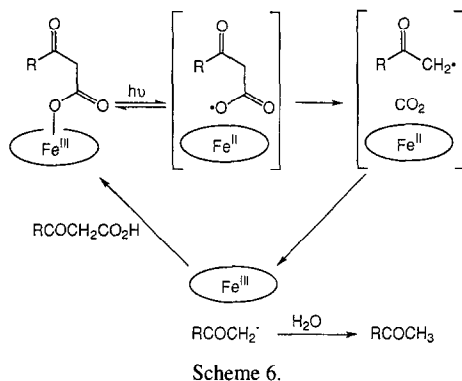

Fig. 6. The EPR spectrum of radical adducts to DMPO formed in the anaerobic photoreaction of Fe^{III}T2MPyP and 3-methyl-2-oxobutanoic acid in aqueous solution. Me_2CHĊO (■) and Me_2ĊH (×).

Scheme 6.

Fig. 7. The time dependent build-up of Fe^{II}T2MPyP in the anaerobic photoreactions of Fe^{III}T2MPyP with malonic acid (●), acetic acid (♦), monoethyl malonate (○), dimethylmalonic acid (■) and 2-methylpropanoic acid (▲) in aqueous solution.

is followed by a rapid one-electron transfer from Fe^{II}T2MPyP to the α-ketoradical within the solvent cage (Scheme 6). The overall effect of this step is to oxidise the Fe^{II}T2MPyP and to make the system catalytic in Fe^{III}T2MPyP.

The photoreaction of the γ-ketoacid, 4-oxopentanoic acid resembles that of an alkylcarboxylic acid, although the CO group reduces the rate of reaction to less than that of acetic acid.

2.5. β-dicarboxylic acid complexes

The photoreduction of Fe^{III}T2MPyP by β-dicarboxylic acids occurs at a comparable but slightly slower rate than that of the analogous alkylmonocarboxylic acid (Fig. 7). The α-methyl groups in 2,2-dimethylmalonic acid enhance the rate of iron(II) formation, presumably in an analogous manner to that observed in the alkylmonocarboxylic acids. Interestingly, the
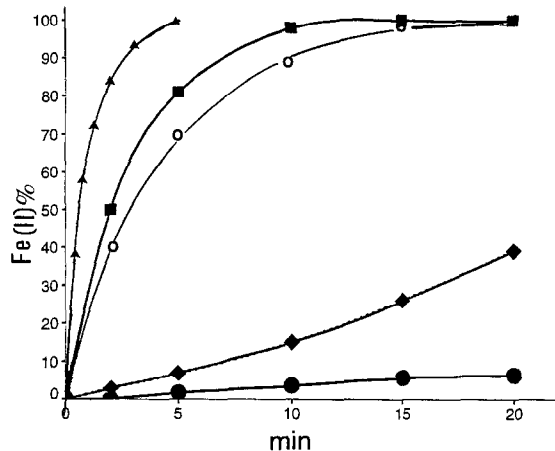
monoethyl ester of malonic acid reacts substantially faster than malonic, suggesting the ester group is better able to stabilise the radical, following decarboxylation, than is a carboxylic acid group.

None of the reactions showed evidence of the catalytic process noted for the β-ketoacid above. In agreement with this observation a ketone is known to be more effective at stabilising an α-carbanion than an ester group (cf. σ^- values of 4-COMe and 4-CO$_2$Me, 0.87 and 0.68, respectively [13]).

Table 3
Catalyst turnovers in the aerobic photoreactions of phenylacetic and phenylpyruvic acid with Fe^{III}T2MPyP and supported Fe^{III}T2MPyP [a]

Catalyst	Carboxylic acid	Solvent	Time (min)	Yield (catalyst turnovers [b])		
				PhCH$_2$OH	PhCHO	PhCH$_2$CH$_2$Ph
Fe^{III}T2MPyP	PhCH$_2$CO$_2$H	H$_2$O	60 [c]	15	133	2
Fe^{III}T2MPyP	PhCH$_2$CO$_2$H	CH$_3$CN	60 [c]	—	387	—
Si–Fe^{III}T2MPyP [d]	PhCH$_2$CO$_2$H	CH$_3$CN	720 [e]	27	932	—
Fe^{III}T2MPyP	PhCH$_2$COCO$_2$H	H$_2$O	5 [f]	—	317	—

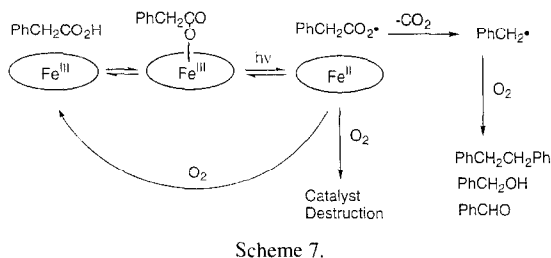[a] [Cat] = 1 × 10^{-5} M; [RCO$_2$H] = 0.1 M.
[b] Moles of product/moles of catalyst.
[c] Catalyst > 90% bleached.
[d] Silica-supported Fe^{III}T2MPyP.
[e] UV–vis spectroscopy indicates negligible photobleaching of catalyst.
[f] Catalyst 30% bleached.

Scheme 7.

Fig. 8. Photodecarboxylation of carboxylic acids using Fe^{III}T2MPyP supported on silica.

2.6. Catalytic oxidative decarboxylation

The potential of the photocleavage of carboxylic acids to be turned into a catalytic system, using dioxygen to regenerate the Fe^{III}T2MPyP, was examined with two substrates, phenylacetic and phenylpyruvic acid, which gave products that could be readily analyzed by GC (Table 3). The major limitation of the system was the oxidative destruction of the iron porphyrin which competed with the desired photocatalytic cycle (Scheme 7). Thus, although the reaction of phenylacetic acid in water gave products expected of the benzyl radical, after ca. 150 turnovers > 90% of the catalyst had been destroyed. Interestingly, the stability of the catalyst was greater in acetonitrile and when phenylpyruvic acid was used as the substrate. The precise cause of the instability of the catalyst is unclear, however, it is likely that oxidative destruction occurs during the regeneration of Fe^{III}T2MPyP from Fe^{II}T2MPyP by dioxygen.

Two mechanisms have been proposed for the iron(II)–iron(III) conversion (Scheme 8), the first (path a) involves the formation of monomeric peroxoiron species which subsequently give HO$_2^-$ radicals [7,14]. In the second
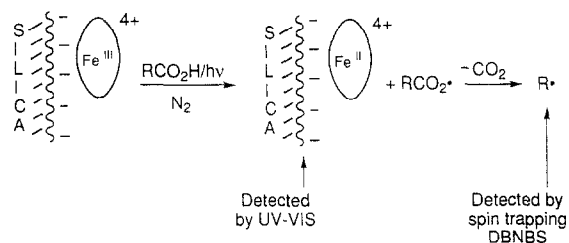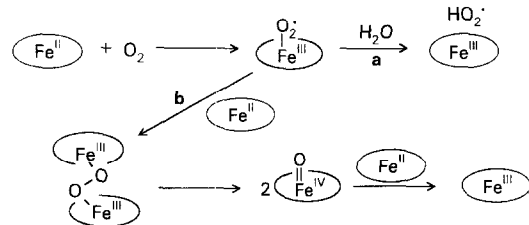
(path b), the peroxoiron species reacts with another iron(II) porphyrin to give a μ-peroxodimer which cleaves to two oxoiron(IV) species [15]. Comproportionation of iron(II) and iron(IV) species regenerates the iron(III) porphyrin.

Oxidative destruction of the porphyrin ring can be envisaged as occurring either by the addition of oxyl-radicals to the porphyrin ring or by an intermolecular porphyrin–porphyrin reaction of the oxoiron(IV) species. In agreement with the latter explanation, the stability of Fe^{III}T2MPyP was dramatically improved when electrostatically bound to silica gel (Fig. 8) [16,17]. After > 900 turnovers, UV–vis spectroscopy showed no evidence for catalyst destruction (Fig. 9). We argue that under these conditions the immobilised iron porphyrin is unable to form μ-peroxodimers, which in turn prevents the formation of oxoiron(IV) species and catalyst bleaching.
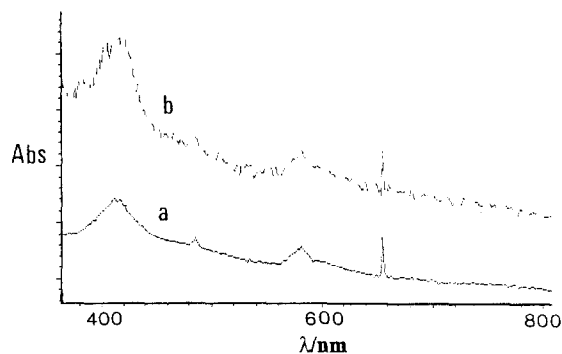

Scheme 8.

Fig. 9. UV–vis spectrum of a suspension of Fe^{III}T2MPyP supported on silica in acetonitrile before (a) and after (b) 12 h aerobic photoreaction with phenylacetic acid.

3. Experimental

3.1. Materials

All materials were commercially available and used without purification unless otherwise stated. DMPO (Sigma) was purified by treatment with activated charcoal before use. DBNBS was prepared from 3,5-dibromosulphanilic acid [18]. $Fe^{III}T2MPyP$ was prepared as described previously [19] and supported on Kieselgel 60 (10 mg of iron(III) porphyrin g^{-1}) [16].

3.2. Instrumentation

The photolyses were carried out using an ILC 302 UV xenon high-intensity source (300 W; $\lambda > 390$ nm) directed by a liquid light guide (Laser Lines). Reactions in the absence of dioxygen were carried out in sealed cuvettes following thorough flushing with dioxygen free nitrogen. UV–vis spectra were recorded with a Hewlett Packard 8452A diode array spectrometer and analyzed with a Hewlett Packard HP9500 UV–vis ChemStation. EPR spectra were obtained using a Bruker ESP 300 spectrometer equipped with 100 kHz modulation and a Bruker ER 035H gaussmeter for field calibration. Product studies were carried out by gas chromatography using a Pye Unicam GCD chromatograph fitted with a flame ionisation detector and a packed column, DEGA (10%, w/w) on Celite (80–120 mesh). The results were recorded and analyzed on a Trivector Trilab 2000 data station. pH measurements were made with a Corning Delta 220 pH meter equipped with a Russell's CE 7L combined pH/reference electrode.

3.3. Photolyses

For UV–vis studies, photolyses of solutions and suspensions used quartz cuvettes (1 cm). Photolyses of solutions for EPR experiments were carried out in situ in an aqueous sample cell. Experiments using suspensions of Si–$Fe^{III}T2MPyP$ were carried out externally and filtered solutions were examined in the EPR spectrometer.

References

[1] L.M. Epstein, D.K. Straub and C. Maricondi, Inorg. Chem. 6 (1967) 1720; J. Del Gaudio and G.N. La Mar, J. Am. Chem. Soc. 100 (1978) 1112; G.S. Srivasta and D.T. Savage, Inorg. Chem. 24 (1985) 1732; C.E. Castro, M. Jarvin, W. Yokoyama and R. Wade, J. Am. Chem. Soc. 108 (1986) 4179; T. Yoshimura, H. Toi, S. Inoba and H. Ogoshi, Inorg. Chem. 34 (1991) 4315; D. Mansuy, Coord. Chem. Rev. 106 (1993) 779; P.R. Cooke, Ph.D. thesis, York, UK (1993).

[2] C. Bizet, P. Molière, D. Brault, O. Delgado, M. Bazin and R. Santus, Photochem. Photobiol. 34 (1981) 315; T. Inamura, T. Jin, T. Suzuki and M. Fujimoto, Chem. Lett. (1985) 847; K.S. Suslick and R. Watson, New J. Chem. 16 (1992) 633.

[3] D.N. Hendrickson, M.G. Kinnaird and K.S. Suslick, J. Am. Chem. Soc. 109 (1987) 1243.

[4] A. Tohara and M. Sato, Chem. Lett. (1989) 153.

[5] C. Bartocci, A. Maldotti, G. Varani, V. Cassitti, P. Battioni and D. Mansuy, J. Chem. Soc. Chem. Commun. (1989) 964.

[6] C. Bartocci, A. Maldotti, G. Varani, P. Battioni and D. Mansuy, Inorg. Chem. 30 (1991) 255.

[7] M. Hoshimo, K. Ueda, M. Takahashi, M. Yamaji and Y. Hama, J. Chem. Soc. Faraday Trans. 88 (1992) 405.

[8] P.E. Ellis and J.E. Lyons, J. Chem. Soc. Chem. Commun. (1989) 1315; P.E. Ellis and J.E. Lyons, Coord. Chem. Rev. 105 (1990) 181; J.E. Lyons and P.E. Ellis, Catal. Lett. 8 (1991) 45; J.E. Lyons and P.E. Ellis, in: Metalloporphyrins in Catalytic Oxidations, R.A. Sheldon (Ed.) (Marcel Dekker, New York, 1994) ch. 10.

[9] Y. Ito, J. Chem. Soc. Chem. Commun. (1991) 622; A. Maldotti, C. Bartocci, R. Armadelli, E. Polo, P. Battioni and D. Mansuy, J. Chem. Soc. Chem. Commun. (1991) 1487; Y. Ito, K. Kurimoto, S. Miyachi and T. Kako, Tetrahedron Lett. 32 (1991) 4007; B.C. Gilbert, J.R. Lindsay Smith, P. MacFaul and P. Taylor, J. Chem. Soc. Perkin Trans. 2 (1993) 2033; B.C. Gilbert, J.R. Lindsay Smith, P. MacFaul and P. Taylor, J. Chem. Soc. Perkin Trans. 2 (1996) 511; B.C. Gilbert, G.R. Hodges, J.R. Lindsay Smith, P. MacFaul and P. Taylor, J. Chem. Soc. Perkin Trans. 2 (1996) 519.

[10] J.W. Hilborn and J.A. Pincock, J. Am. Chem. Soc. 113 (1991) 2683.

[11] H. Goff and M.G. Simic, Biochim. Biophys. Acta. 392 (1975) 201; D. Brault, C. Bizet, P. Molière, M. Rougee, E.J. Land, R. Santus and A.J. Swallow, J. Am. Chem. Soc. 102 (1980) 1015.

[12] J. Fossey, D. Lefort and J. Sorba, Free Radicals in Organic Chemistry (Wiley, Chichester, 1995) p. 297.

[13] C.D. Ritchie and W.F. Sager, Prog. Phys. Org. Chem. 1 (1963) 35.

[14] M. Momenteau and C.A. Reed, Chem. Rev. 94 (1994) 659.

[15] D.H. Chin, A.L. Balch and G.N. LaMar, J. Am. Chem. Soc. 102 (1980) 1446; A.L. Balch, Y.-W. Chan, R.-J. Cheng, G.N. LaMar, L. Latos-Grazynski and M.W. Renner, J. Am. Chem. Soc. 106 (1984) 7779.

[16] P.R. Cooke and J.R. Lindsay Smith, J. Chem. Soc. Perkin Trans. 2 (1994) 1913.

[17] P.R. Cooke, C. Gilmartin, G. Gray and J.R. Lindsay Smith, J. Chem. Soc. Perkin Trans. 2 (1995) 1573.

[18] K. Kaur, H.W. Leung and M.J. Perkins, J. Chem. Soc. Chem. Commun. (1981) 142.

[19] D.R. Leanord and J.R. Lindsay Smith, J. Chem. Soc. Perkin Trans. 2 (1990) 1917.